Full-field X-ray microscopy with crossed partial multilayer Laue lenses

Sven Niese,[1,2,*] Peter Krüger,[1] Adam Kubec,[3,4] Stefan Braun,[4] Jens Patommel,[5] Christian G. Schroer,[5] Andreas Leson,[4] and Ehrenfried Zschech[1,2]

[1]*Fraunhofer IKTS Dresden, Winterbergstrasse 28, 01277 Dresden, Germany*
[2]*Technische Universität Dresden, Dresden Center for Nanoanalysis, 01062 Dresden, Germany*
[3]*Institute for Materials Science and Max Bergmann Center of Biomaterials, Technische Universität Dresden, 01062 Dresden, Germany*
[4]*Fraunhofer IWS Dresden, Winterbergstrasse 28, 01277 Dresden, Germany*
[5]*Technische Universität Dresden, Institut für Strukturphysik, 01062 Dresden, Germany*

[*]*roentgen@ikts-md.fraunhofer.de*

Abstract: We demonstrate full-field X-ray microscopy using crossed multilayer Laue lenses (MLL). Two partial MLLs are prepared out of a 48 µm high multilayer stack consisting of 2451 alternating zones of WSi_2 and Si. They are assembled perpendicularly in series to obtain two-dimensional imaging. Experiments are done in a laboratory X-ray microscope using Cu-Kα radiation ($E = 8.05$ keV, focal length $f = 8.0$ mm). Sub-100 nm resolution is demonstrated without mixed-order imaging at an appropriate position of the image plane. Although existing deviations from design parameters still cause aberrations, MLLs are a promising approach to realize hard X-ray microscopy at high efficiencies with resolutions down to the sub-10 nm range in future.

© 2014 Optical Society of America

OCIS codes: (050.1965) Diffractive lenses; (340.7460) X-ray microscopy.

References and links

1. A. Tkachuk, M. Feser, H. Cui, F. Duewer, H. Chang, and W. Yun, "High-resolution x-ray tomography using laboratory sources," in *Optics & Photonics* (International Society for Optics and Photonics, 2006), p. 63181D-1.
2. J. Maser, G. B. Stephenson, S. Vogt, W. Yun, A. Macrander, H. C. Kang, C. Liu, and R. Conley, "Multilayer Laue lenses as high-resolution x-ray optics," in *Proc. SPIE* vol. 5539 (2004), p. 185.
3. H. Kang, J. Maser, G. Stephenson, C. Liu, R. Conley, A. Macrander, and S. Vogt, "Nanometer linear focusing of hard x rays by a multilayer Laue lens," Phys. Rev. Lett. **96**, 127401 (2006).
4. T. Liese, V. Radisch, and H. Krebs, "Fabrication of multilayer Laue lenses by a combination of pulsed laser deposition and focused ion beam," Rev. Sci. Instrum. **81**, 073710 (2010).
5. H. Yan, V. Rose, D. Shu, E. Lima, H. C. Kang, R. Conley, C. Liu, N. Jahedi, A. T. Macrander, G. Stephenson, M. Holt, Y. S. Chu, M. Lu, and J. Maser, "Two dimensional hard x-ray nanofocusing with crossed multilayer Laue lenses," Opt. Express **19**, 15069 (2011).
6. D. Attwood, *Soft X-Rays and Extreme Ultraviolet Radiation* (Cambridge University Press, 1999).
7. H. Yan, H. C. Kang, R. Conley, C. Liu, A. T. Macrander, G. B. Stephenson, and J. Maser, "Multilayer Laue lens: a path toward one nanometer x-ray focusing," X-ray Opt. Instrum. **2010**, 401854 (2010).
8. C. G. Schroer, "Focusing hard x rays to nanometer dimensions using Fresnel zone plates," Phys. Rev. B **74**, 033405 (2006).
9. K. Jefimovs, J. Vila-Comamala, T. Pilvi, J. Raabe, M. Ritala, and C. David, "Zone-doubling technique to produce ultrahigh-resolution x-ray optics," Phys. Rev. Lett. **99**, 264801 (2007).
10. W. Chao, B. D. Harteneck, J. A. Liddle, E. H. Anderson, and D. T. Attwood, "Soft x-ray microscopy at a spatial resolution better than 15 nm," Nature **435**, 1210 (2005).

#212412 - $15.00 USD Received 22 May 2014; revised 25 Jun 2014; accepted 1 Jul 2014; published 12 Aug 2014

11. Y. Feng, M. Feser, A. Lyon, S. Rishton, X. Zeng, S. Chen, S. Sassolini, and W. Yun, "Nanofabrication of high aspect ratio 24 nm x-ray zone plates for x-ray imaging applications," J. Vac. Sci. Technol., B: Microelectron. Nanometer Struct. **25**, 2004 (2007).
12. S. Werner, S. Rehbein, P. Guttman, S. Heim, and G. Schneider, "Towards stacked zone plates," in *J. Phys.: Conf. Ser.*, vol. 186 (IOP Publishing, 2009), p. 012079.
13. S. Braun and H. Mai, *Metal Based Thin Films for Electronics* (Wiley-VCH, 2006), chap. Multilayers for x-ray optical purposes, p. 309.
14. S. Braun, A. Kubec, M. Menzel, S. Niese, P. Krüger, F. Seiboth, J. Patommel, and C. G. Schroer, "Multilayer Laue lenses with focal length of 10 mm," in *J. Phys.: Conf. Ser.*, vol. 425 (IOP Publishing, 2013), p. 052019.
15. Root mean square value of roughness σ_r and interdiffusion σ_i: $\sigma = (\sigma_\mathrm{r}^2 + \sigma_\mathrm{i}^2)^{0.5}$
16. S. Niese, P. Krüger, A. Kubec, R. Laas, P. Gawlitza, K. Melzer, S. Braun, and E. Zschech, "Fabrication of customizable wedged multilayer Laue lenses by adding a stress layer," Thin Solid Films (2014). http://dx.doi.org/10.1016/j.tsf.2014.02.095, in press.
17. W. Rasband, "ImageJ, U. S. National Institutes of Health, Bethesda/MD, USA," http://imagej.nih.gov/ij/ (2014).
18. A. Schropp, P. Boye, J. M. Feldkamp, R. Hoppe, J. Patommel, D. Samberg, S. Stephan, K. Giewekemeyer, R. N. Wilke, T. Salditt, J. Gulden, A. P. Mancuso, I. A. Vartanyants, E. Weckert, S. Schoder, M. Burghammer, and C. G. Schroer, "Hard x-ray nanobeam characterization by coherent diffraction microscopy," Appl. Phys. Lett. **96**, 091102 (2010).
19. S. Hönig, R. Hoppe, J. Patommel, A. Schropp, S. Stephan, S. Schöder, M. Burghammer, and C. Schroer, "Full optical characterization of coherent x-ray nanobeams by ptychographic imaging," Opt. Express **19**, 16324 (2011).

1. Introduction

X-ray microscopy (XRM) has become a powerful technique to investigate nanoscale structures and kinetic processes at synchrotron radiation facilities and in laboratories [1] using X-ray lenses for optical imaging. Thus, the gap in spatial resolution for transmission imaging and tomography between microfocus X-ray radiography and transmission electron microscopy can be filled. Fresnel zone plates (FZP) represent the state of the art X-ray lenses, whereas multilayer Laue lenses (MLL) are an emerging approach for new X-ray optics [2]. Recent studies at synchrotron radiation facilities solely investigated the focusing properties of MLLs [3–5]. Their imaging capabilities were not exploited so far experimentally to our knowledge.

Both lens types, FZPs and MLLs, are diffractive optics consisting of alternating regions of materials with different refractive indices, and a single MLL can be understood as a linear zone plate. The resolution for first order imaging is limited by the width of the outermost zone Δr_n [6]. It is $1.22\Delta r_n$ and Δr_n for a *complete* FZP and MLL, respectively. The value increases in case of a *partial* MLL – i.e. not all zones are deposited – due to the decreased numerical aperture. The resolution is obtained by $0.5\lambda f/h$, if the wavelength λ, the height of the multilayer stack h, and the focal length f are known. Diffraction efficiency can be enhanced, if the absorption of the zones is minimized and if the relative phase shift resulting from the propagation through adjacent zones with different refractive indices equals π. In particular for hard X-rays, the corresponding length of the zones along the optical axis increases to several microns and volume diffraction effects occur. This effect is exploited in wedged and curved MLLs where each zone is placed in Bragg condition. In case of zone widths $\lesssim 20\,\mathrm{nm}$, the diffraction efficiency exceeds the limit of 40 % that is given for first order focusing of a thin phase zone plate [7]. Furthermore, it is mandatory to fulfill the Bragg condition to focus X-rays to single nanometers since volume diffraction otherwise limits the resolution [8]. It is expected that this approach is not entirely suitable for imaging an extended object with such ultimate resolution because the field of view that is accepted by the lens is too small [8]. However, this restriction applies for MLLs and FZPs, whereas MLLs offer better experimental capabilities to approach 5 nm resolution, which is an expected limit for focusing with tilted MLLs [3].

The desired high aspect ratios exceed the current limits of zone plate fabrication based on electron beam lithography and subsequent etching [9, 10]. Approaches like zone plate stacking push the limits only slightly further [11, 12]. As a major advantage, MLL optics do not have any upper bounded aspect ratio limitation since they are cut out of a multilayer stack, manufactured

#212412 - $15.00 USD Received 22 May 2014; revised 25 Jun 2014; accepted 1 Jul 2014; published 12 Aug 2014
(C) 2014 OSA

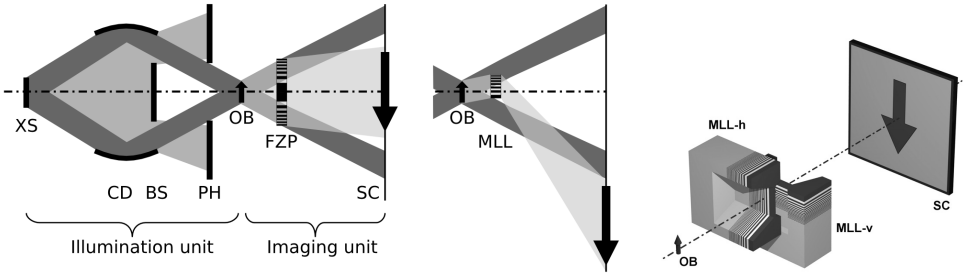

(a) FZP (b) MLL (c) visualization

Fig. 1. (a) Scheme of the optical path. The illumination unit consists of the X-ray source (XS), a capillary condenser (CD) with a beamstop (BS) and a pinhole (PH). The object (OB) is imaged by the Fresnel zone plate (FZP) to the scintillating screen (SC). Hollow cone illumination is shown in dark gray. (b) Imaging unit using a partial multilayer Laue lens (MLL). (c) Scheme of crossed MLLs after FIB preparation and assembly used to image an object (OB) to the screen (SC). MLL-h and MLL-v are the horizontally and vertically imaging lens, respectively.

by thin film deposition [4]. The thicknesses of those layers follow the zone plate law, and layer thicknesses down to 1 nm can be produced with high quality [13]. The thinnest layers are deposited directly onto the substrate, as they have the highest requirements regarding roughness and thickness [14], and zones beyond the optical axis are usually omitted at the layer deposition, which leads to a half lens. Subsequently, two of these partial MLLs are assembled in series to get a lens operating two-dimensionally. Figure 1(c) illustrates the imaging unit of an X-ray microscope containing two crossed partial MLLs, as used in the experiments described here.

2. MLL fabrication

The multilayer stack with a total height of $h = 47.9\,\mu\text{m}$ was fabricated by alternate magnetron sputter deposition of amorphous silicon and tungsten disilicide (WSi_2), respectively, onto a silicon wafer. The deposition time was 53 h. The layers show low interface widths σ of $0.3 - 0.4$ nm RMS [15]. The stack contains zone numbers 2500 to 50, what corresponds to individual layer thicknesses of 11 nm to 79 nm. For such an MLL, the focal length at $E = 8.0$ keV is designed to be $f = 8.0$ mm, and the theoretically achievable resolution based on this aperture is 26 nm. The deposition process was controlled in a way that a radial thickness gradient was produced on the wafer. Therefore, vertically and horizontally focusing lenses with matching focal lengths can be cut from a single wafer at selected distances from the wafer center. Subsequently, the lens element itself was prepared by focused ion beam (FIB) milling similar to the H-bar preparation of lamellae for transmission electron microscopy [16]. FIB processing took about 3 hours at 27 nA Ga^+ beam current, resulting in a lens of 60 µm width and 4.5 µm thickness. Since both deposited materials are amorphous, no curtaining artifact occurred during milling of the sidewalls. To achieve crossed MLLs, two partial lenses were directly bonded onto each other. The angular alignment error was determined to be less than 0.15 °.

3. Description and simulation of the bright field of an MLL

The imaging tests were performed in a laboratory X-ray microscope *NanoXCT-100* (Xradia, Pleasanton/CA, USA; [1]). Its optical path is sketched in Fig. 1(a). The illumination unit consists of an X-ray tube with a rotating copper anode and a capillary condenser, which transfers the focus of the anode to a hollow cone illumination of the object plane, as well as a beam-

#212412 - $15.00 USD Received 22 May 2014; revised 25 Jun 2014; accepted 1 Jul 2014; published 12 Aug 2014
(C) 2014 OSA

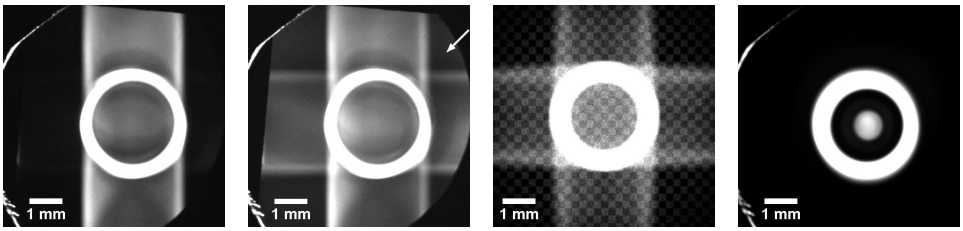

(a) single MLL (b) crossed MLLs (c) simulation (d) FZP

Fig. 2. MLL bright field of a (a) single partial and (b) crossed partial MLLs acquired on the larger scintillating screen. The field of view exceeds the condenser ring. In case of crossed MLLs, there appears some intensity in the corners. The arrow in (b) marks the position, where full-field images were acquired. (c) Geometrical optics simulation using crossed cylindrical lenses with a limited efficiency of 35 % (d) The same screen showing the zone plate's bright field surrounded by the condenser ring.

stop and a pinhole to stop direct beams. Although there is no strict monochromatizing element, imaging is dominated by the Cu-Kα radiation ($E = 8.05\,\mathrm{keV}$). Cu-Kβ radiation can be suppressed using a 10 µm thick nickel filter. An FZP images the object to a scintillating screen, and subsequently the image is magnified by a visible light microscope to a CCD camera. On the larger scintillating screen, the actual image of the FZP is surrounded by zero-order beams of the hollow cone illumination, which we call condenser ring, see Fig. 2(d). A smaller scintillating screen serves as a high-resolution image detector to acquire the actual micrographs.

The crossed MLLs were mounted inside the microscope and coarsely aligned using the built-in FZP. Obviously, bright field images from MLL and FZP differ significantly. Figure 2(a) depicts the bright field image of a single MLL, corresponding to MLL-v in Fig. 1(c). For visualization, gray scales are chosen for best contrast of the MLL effect, which leads to an overexposure of the dominating condenser ring. As it can be derived for a one-dimensional imaging lens, the first-order image of the hollow cone illumination appears as a very long ellipse onto the detector due to the large magnification of 93×, where only the central part is visible.

In case of crossed MLLs, a second stripe appears, corresponding to the imaging direction of the other MLL, see Fig. 2(b). At first glance, it seems that both MLLs provide independent images, as there are two individual stripes visible instead of one large bright field image. Indeed, following the straightforward approach based on the FZP setup we did not achieve a micrograph of an object in the center of the condenser ring due to mixed order images of both serial lenses at this position. However, there is some intensity noticeable in the corners of the image plane outside both stripes. These regions are exclusively illuminated by first-order images of both lenses. Using two partial MLLs that show a useful point-spread-function predominantly on one side of the optical axis, there is one distinctive corner where a proper image can be expected, see Fig. 1(b) and the arrow in Fig. 2(b). Eventually, the high-resolution image of the object was found there, and the small scintillating screen was moved to this position.

In addition, the appearance of the bright field was simulated using geometrical optics. The simulation considers all optical components shown in Fig. 1. Dimensions of all elements were set to known values – e.g. for the sizes of the X-ray source, pinhole, and screen as well as for the positions of all elements along the optical axis – or estimated – particularly the geometry of the capillary condenser. The crossed MLLs were replaced by two crossed cylindrical lenses with the same focal length. The probability that an incident ray is accordingly refracted is set to 35 % to account for the limited diffraction efficiency of each MLL. A chessboard-like grid of totally transparent and absorbing regions is placed in the object plane. The resulting image

#212412 - $15.00 USD Received 22 May 2014; revised 25 Jun 2014; accepted 1 Jul 2014; published 12 Aug 2014
(C) 2014 OSA

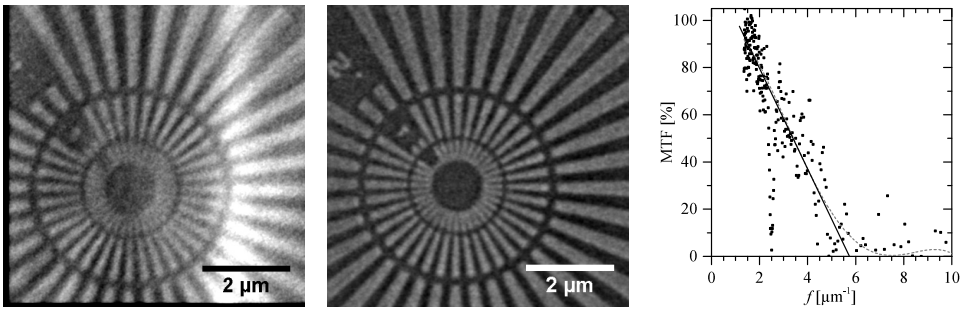

(a) MLL (b) FZP (c) MTF

Fig. 3. Micrographs of the center of the Siemens star pattern acquired (a) with the MLL and (b) with the FZP as reference. (c) Modulation transfer function (MTF) of (a), determined at concentrical intensity profiles. 10 µm^{-1} corresponds to 50 nm lines and spaces.

at the position of the scintillating screen is shown in Fig. 2(c). The simulation is in agreement with the observed bright field of the crossed partial MLLs. Mixed order imaging in the center of the condenser ring and at the position of both stripes is clearly seen, i.e. the image of the grid is overlaid by a significant background. Proper imaging is recognized in all four corners due to the use of complete cylindrical lenses.

4. Full-field imaging experiments

The imaging performance is demonstrated at an X-ray resolution target, possessing a Siemens star pattern with a minimum feature size of 50 nm, patterned by etching into a 500 nm thick Ta absorber (*NTT-AT ATN/XRESO-50HC*, NTT-AT, Tokyo, Japan). The object illumination is truncated by a 12×33 µm^2 pinhole. For comparison, radiographs are acquired with the high-resolution FZP and the 60 µm pinhole belonging to the X-ray microscope. The latter image is cropped and scaled to fit the field of view of the MLL. Averaged reference images are obtained by the *Despeckle and Average* function in *XMController 9.0* (Xradia, Pleasanton/CA, USA). Further image processing was done in ImageJ [17]. All micrographs are reference corrected and subsequently aligned, averaged, and processed with a 1.0 px Gaussian filter.

Figure 3(a) shows a micrograph of the center of the Siemens star pattern. Due to a continuous slow drift of the lens during the image acquisition, a drift correction procedure was applied. Thus, the micrograph suffers an uneven bright field reference. From the visual impression, the resulting micrograph resolves sub-100 nm features and it almost achieves the resolution of the FZP, see Fig. 3(b). The cut-off frequency f was determined with a modulation transfer function calculation at Fig. 3(a) to be 5.75 µm^{-1}, see Fig. 3(c). This corresponds to a resolution of 87 nm. Focus series of the specimen indicate a focus offset of about 20 µm for the vertical and horizontal imaging MLL, leading to a degraded resolution at the chosen intermediate position.

For Fig. 3(a), 16 micrographs each collected in 450 s at binning 2 (512×512 px) using the 10 µm nickel filter were acquired for both, image and reference. All individual micrographs were aligned by a linear translation of at most 16 pixels in horizontal and 10 pixels in vertical direction before averaging. The pixel size of the micrograph was calculated to 13.4 nm at binning 2. For Fig. 3(b), 16 micrographs each collected in 450 s at binning 1 (1024×1024 px) without Ni filter were acquired for image and reference. A drift correction of at most 4 px in horizontal direction was applied.

To quantify further properties like contrast and efficiency, a position of the Siemens star containing broader lines was selected (Fig. 4). Striking in the micrograph obtained with the

#212412 - $15.00 USD Received 22 May 2014; revised 25 Jun 2014; accepted 1 Jul 2014; published 12 Aug 2014
(C) 2014 OSA

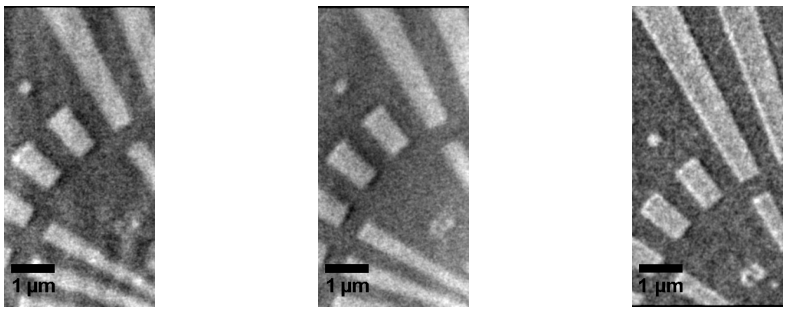

5.8%, 8569 cts/µm^2/s (a) MLL

8.8%, 3754 cts/µm^2/s (b) MLL + Ni filter

5.6%, 5121 cts/µm^2/s (c) FZP

Fig. 4. Micrograph of an area with coarse features that is used for contrast calculation. (a) MLL, (b) MLL with 10 µm nickel filter, (c) FZP. Gray scales are set to transmission values of $0.85-1.03$ in (a) and (c), and to $0.80-1.08$ in (b).

MLL is a kind of ghost image of the star pattern that overlays the real image in Fig. 4(a). It can be efficiently suppressed using the nickel filter as shown in Fig. 4(b). Thus we deduce that the ghost image is caused by Cu-Kβ radiation ($E = 8.90$ keV). Absorption contrast is calculated based on measured intensities of reference corrected images in adjacent areas with and without Ta. The calculated absorption of 500 nm Ta at 8.05 keV equals 12.3 %. The contrast without filter is equivalent to that for the FZP, cf. Fig. 4(c). However, an even better value was observed using the filter. As a measure of efficiency, the normalized flux of the bright field was calculated. At the same conditions, crossed MLLs collect two thirds more photons than the commercially available FZPs. Applying the filter, the value decreases to three quarters of the FZP flux.

5. Conclusion

To summarize, we showed that crossed partial multilayer Laue lenses can be integrated into a laboratory X-ray microscope for full-field imaging with hard X-rays by accepting an image formation aside the natural optical path of the microscope. The tight assembly of both individual partial MLLs to a single lens element yields a practical solution for lens adjustment inside the microscope and provides a virtually undistorted image due to a focal length variation of less than 0.5 %. We observe sub-100 nm resolution at competitive contrast and efficiency values using the MLL setup described in this paper. The assembly has a shorter focal length and it requires a nickel filter to suppress ghost images. To improve the MLL optics further, a more detailed characterization by ptychography [18, 19] at synchrotron facilities was done. Preliminary results indicate that the generated focus contains undesirable secondary peaks due to drifts of the deposition rate and imperfections of the assembly, which have to be suppressed in the future. This study demonstrated that multilayer Laue lenses are a very promising approach to improve resolution and efficiency in hard X-ray full-field microscopy, which opens new experimental possibilities to approach theoretical limits.

Acknowledgments

This research was supported by the German Federal Ministry of Research and Education (BMBF) within the CoolSilicon cluster via project CoolAnalytics (SAB grant 75702/2583), and the European Union and the Free State of Saxony via ESF project 100087859, ENano.

#212412 - $15.00 USD Received 22 May 2014; revised 25 Jun 2014; accepted 1 Jul 2014; published 12 Aug 2014
(C) 2014 OSA